Effect of Humpback Whale-Like Leading Edge Protuberances On the Low-Reynolds Number Airfoil Aerodynamics

M.M. Zhang*, G.F. Wang, J.Z. Xu
Institute of Engineering Thermophysics, Chinese Academy of Sciences, Beijing 100190, China
**Corresponding Author, E-mail: mmzhang@mail.etp.ac.cn; Tel: 86-10-82543023*

Extended Abstract

Aerodynamic of airfoils operated at a low chord Reynolds number, i.e. $10^4 < Re_c < 10^5$, has recently gained an increasingly importance within a variety of application fields, such as micro air vehicles (MAVs), small unmanned air vehicles (UAVs), low-speed/high-altitude aircraft and small wind turbines. Nevertheless, the airfoils in this low Re_c range are often subject to flow separation and even stall, resulting in poor aerodynamic performances and shortened fatigue lives of the above-mentioned engineering structures. Therefore, effective control methods must be taken to improve this kind of airfoil aerodynamics.

Recently, a new type of passive control method, so called leading-edge protuberance, has been paid more and more attention and the idea was inspired by the humpback whale flipper with rounded tubercles interspersed along its leading-edge, which enables the giant humpback whale to execute complex underwater rolls, loops and pursuit of preys. Within last decade, many research works have been performed to investigate the effects of tubercles on the airfoil aerodynamic and hydrodynamic and good performances have been reported. Even so, the detailed understanding of flow physics behind is still very lack, which may blockage the technique to be applied in the future. To this end, this paper presents an experimental study to investigate the nature of the modified airfoil aerodynamics by the presence of protuberances at low Re_c.

Experiments were conducted in an open-loop wind tunnel with a test section of 0.5 (width) × 0.5 m (height) × 2 m (length) at Tsinghua University. The detailed setup was shown in Fig.1. Two rectangular aluminum full-span NACA63_4-021 airfoils, i.e. a wavy airfoil with a sinusoidal leading edge (mimicking the cross section to the flipper of humpback whale) and a baseline airfoil with smooth leading edge, were chosen to be the test models. The angle (α) of attack, positive in the clockwise direction from top view, was varied from 0° to 90°. Measurements were carried out at a typical freestream velocity U_∞=7.5 m/s, corresponding to the Reynolds number Re_c of 5.0×10^4 for all the data herein.

Figure 2 present the dependences of the blockage-corrected lift coefficient (C_L), drag coefficient (C_D) and lift-to-drag ratio L/D, on α. The stall occurred at $\alpha = 13^\circ$ and then C_L displays another maximum at $\alpha = 45^\circ$. Compared with the baseline airfoil, all aerodynamic coefficients tend to be stable up to $\alpha = 3^\circ$. After that, as $3^\circ < \alpha \leq 16^\circ$, C_L and L/D evidently decrease [Fig. 2(a) and 2(c)] while C_D mildly increases [Fig. 2(b)]; the flow for the wavy airfoil case seems to not stall in the traditional sense of a rapid increase and thereafter a significant decrease in C_L, but C_L gradually increases with α, indicating that the effectiveness of the passive control on inhibiting stall. The analogical phenomena on impairing the stall as well as detrimental to airfoil aerodynamic at the same time by leading edge protuberances were also observed by many previous researchers at the order of Re_c magnitude of 10^5. Moreover, the wavy airfoil exhibits a rather good aerodynamic characteristics even when α varies from 16° to 70°, resulting in maximum 25.0% and 39.2% increase in C_L and L/D, respectively, and maximum 20.0% decrease in C_D, indicated in Figs. 2(a)-2(c).

Figure 3 shows the contours of time-mean vorticity in x-y plane out of 500 PIV images at $\alpha = 13^\circ$. The images for wavy airfoil cases were individually captured through the neighboring trough and peak locations, which are near the airfoil mid-span. Clearly, flow separates at about 1/3c from the leading edge of the baseline airfoil. Once the wavy airfoil is introduced, the situations are much different. Compared with the baseline case, flow in the trough-plane separates a little earlier while flow in the peak-plane adheres to the suction surface

longer. Moreover, the separated flow in the trough-plane reattaches to the suction surface and then moves towards the trailing edge for a while before leaving the surface again, resulting in much stronger separation than the baseline airfoil. Recalling that aerodynamic of the wavy airfoil becomes worse in contrast to the baseline airfoil in the stall region (Figs. 2(a)-2(c), $3^\circ < \alpha \leq 16^\circ$), it implies that the subsequently enhanced separation originated from the complicated flow modification in the trough-plane might be responsible for the worse airfoil performance. This may further change the original variation of C_L with α, leading to the impairment of airfoil stall. On the other hand, for high α case (not shown), although the flow in the trough-plane tends to separate from the leading edge a little more serious than the baseline case, the flow in the peak-plane still attaches the suction side for a rather long distance, which may play a critical role in the improvements for post-stall airfoil aerodynamics. Due to limited space, the detailed analysis of the corresponding velocity field and boundary layer flow would be illustrated in the coming full length paper.

Keywords: aerodynamics; airfoil; leading-edge protuberance; stall; post-stall;

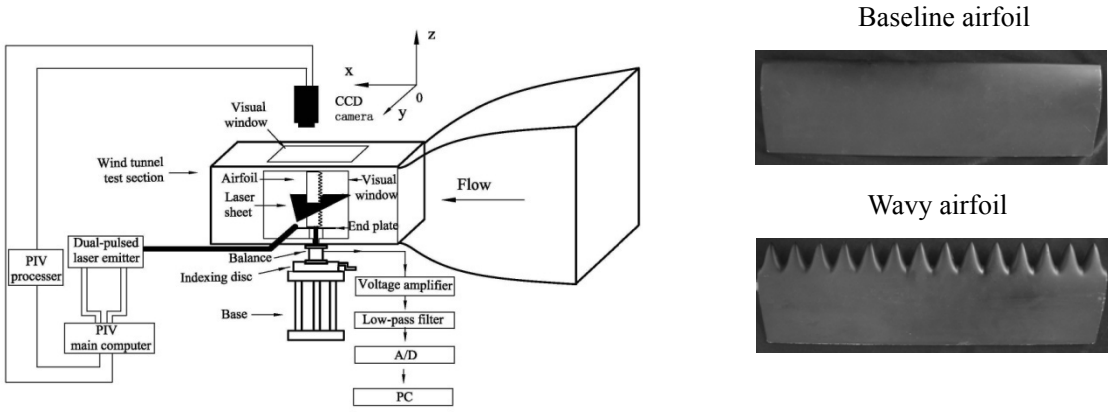

Fig 1. Experimental setup

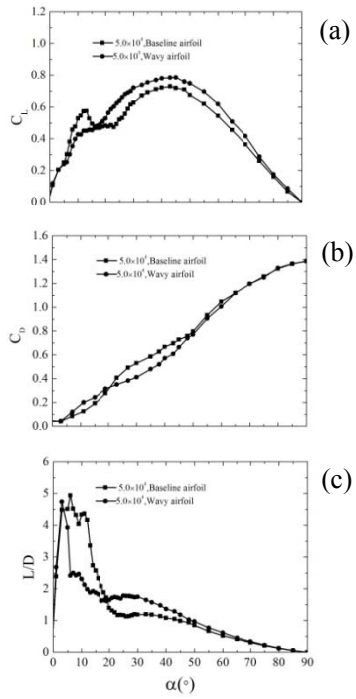

Fig 2. Airfoil aerodynamics with and without control.

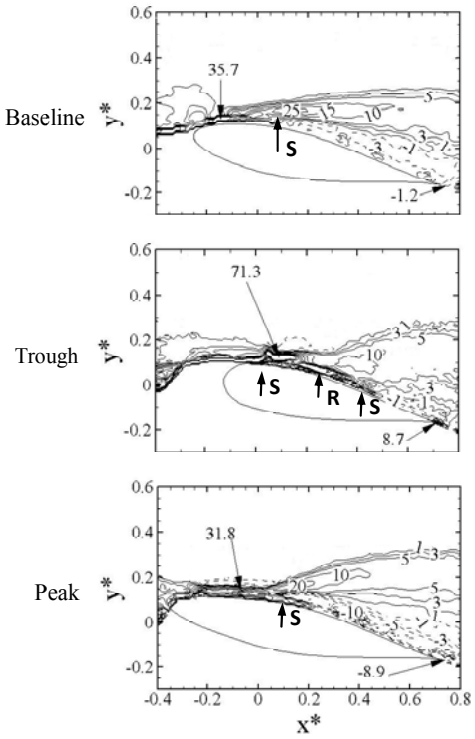

Fig 3. PIV vorticity contour.